Switching Motion Control of the Climbing Robot for Aircraft Skin Inspection

Congqing Wang
College of Automation Engineering
Nanjing University of Aeronautics and Astronautics
Nanjing,China
cqwang@nuaa.edu.cn

Jiayue Gu
College of Automation Engineering
Nanjing University of Aeronautics and Astronautics
Nanjing,China
15852925626@163.com

Zhiyu Li
College of Automation Engineering
Nanjing University of Aeronautics and Astronautics
Nanjing,China
skyfly@nuaa.edu.cn

***Abstract*—In this paper, a climbing robot for aircraft skin inspection with the inner frame and outer frame is developed. The climbing robot carrying a CCD camera can stably adsorb and move on the aircraft surface. The switching motion analysis of the inner frame and outer frame for the climbing robot is given. Motion constraint and dynamics equation are derived. The pneumatic system is designed and used to control the cylinders and suckers. An absorption force control scheme based on a fuzzy control and a feed-forward compensation control using least squares support vector regression(LS-SVR) prediction model is proposed to adjust the pressure difference in the suckers. This fuzzy control ensures that the stable absorption force is maintained even if some disturbance and noises exist. The switching motion and absorption force experiments are carried out and the results of the image inspection show the good performance of non-destructive inspection on airplane.**

***Keywords*—switching motion, climbing robot, fuzzy control, LS-SVR prediction model, aircraft skin inspection**

I. INTRODUCTION

Climbing robots have been applied to unfriendly and dangerous work environments for human beings. A crack inspection system was designed for concrete structures consisting of a mobile robot and a crack detection device [1].The system can provide crack information to evaluate the safety of concrete. The mobile robot used image processing to extract crack information from captured images. The result showed that the system was effective in an indoor structure, a road tunnel, and a subway tunnel. An OmniClimber-II climbing robot [2] with high maneuverability was designed for inspection of ferromagnetic 3D curved environment. Some climbing robots have been used in aircraft skin inspection [3]. Carnegie Mellon University[4] designed a robot using eddy current sensors in application of the aircraft skin inspection. [5] described the development of an universal inspection robot designed to climb on an aircraft surface using Non-Destructive Inspector and perform fuselage inspection automatically. The similar work [6] has been done on acquiring crack images of the aircraft skin by a robot with 3D-stereoscopic video instrumentation for visual inspection. The experimental results showed the robot was able to move along the fuselage on a Boeing 737 aircraft in different spatial orientations. In [7],an automated system that inspects the external surface of an aircraft section was developed. The inspection system was based on a robot carrying a headset made up of ultrasound sensors. Data are processed by an ultrasound processing program which maps the mechanical features of the inspected external surface of the fuselage of an aircraft. The disturbances and noises are often inevitable in robot systems. In [8], authors combined a conventional PI (proportional–integral) controller and a fuzzy PI tuner as the force controller in a robot system for assisting in the rehabilitation of patients. The fuzzy PI tuner was used to compensate for the unknown disturbing force in the robot.

In [9], a stable fuzzy state-feedback controller for a flexible link robotic arm was proposed. The controller was designed on the basis of a neuro-fuzzy state-space model that was trained using real experimental data from the sensors. The controller designed has been successfully implemented for a real robotic arm.

In this paper, a climbing robot for aircraft skin inspection is introduced and switching movement analysis is given. This paper makes the following contributions:

1)The pneumatic system of the climbing robot adjusted by PWM duty cycles.

2) The absorption force control combining the fuzzy control and the feed-forward compensation control using the SVR prediction model.

978-1-5386-1728-1/19/$31.00 ©2019 IEEE

The paper is organized as follows. The climbing robot is described in Section 2. Kinematics and dynamics are analyzed in Section 3. The pneumatic system and absorption force controller are designed in Section 4. Experimental results are given in Section 5. Finally, Section 6 draws the concluding remarks.

II. STRUCTURE OF THE CLIBING ROBOT

Fig. 1(a) shows the climbing robot with the outer frame and the inner frame. The sliding movement between the outer frame and the inner frame can be realized by synchronous leading screw control of a step motor connecting the double frames. The rotating movement can be realized by a step motor in longitudinal direction. The posture of the robot can been adjusted by eight mechanical legs, in which the cylinders are installed. Each leg is equipped with a vacuum sucker. In Fig. 1(b), $OXYZ$ is the base coordinate system, $O_1X_1Y_1Z_1$ is the attached coordinate system , O_1 is the geometry center of the outer frame and the inner frame, β is the rotation angle between the outer frame and the inner frame, v_1 is the sliding velocity, τ_s and τ_r are the driving torques produced by the rotating step motor and the sliding step motor respectively, F_{n1}, F_{n2} are the support forces , F_{a1}, F_{a2} are the adsorption forces, G is the gravity of the robot. $F_{f_i}(i=1,2)$ is the frictional force on the ith sucker. ω_1 is the angular velocity of the rotating step motor.

(a)

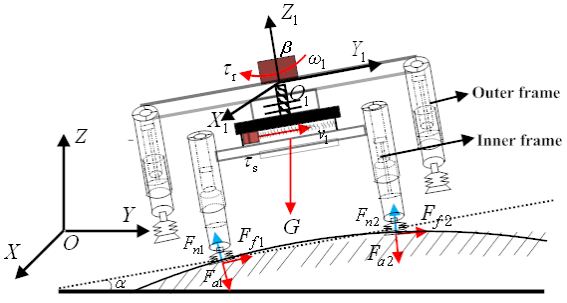

(b)

Fig. 1 Climbing robot with double frame for aircraft skin inspection.

Fig.1 shows the movement of the outer frame when the inner frame adsorbs on surface of an aircraft. In the process of motion, the movement of the inner frame and the outer frame is synchronously switched. The switching motion of the climbing robot was carried out on the fuselage of the aircraft.

A. The Motion Constraint

Considering surface constraint condition of the robot on the aircraft, the dynamic model of the climbing robot with double frame is established by using the Newton-Euler method in the following section. As shown in Fig. 1, the robot moves on a curvature surface with a dip angle α. During the absorption and release of the vacuum suckers of the robot, the velocities in the base coordinate system are given by

$$\begin{cases} \dot{x} = v\sin\beta \\ \dot{y} = v\cos\beta\cos\alpha \\ \dot{z} = v\cos\beta\sin\alpha \end{cases} \tag{1}$$

Based on (1), we can obtain

$$\sin\beta\left(\dot{y}\cos\alpha + \dot{z}\sin\alpha\right) = v\cos\beta\sin\beta = \dot{x}\cos\beta \tag{2}$$

Thus，the motion constraint equation is

$$\boldsymbol{A}(\boldsymbol{q})\dot{\boldsymbol{q}} = \left[-\cos\beta \quad \cos\alpha\sin\beta \quad \sin\alpha\sin\beta \quad 0\right]\left[\dot{x} \quad \dot{y} \quad \dot{z} \quad \dot{\beta}\right]^{\mathrm{T}} = 0 \tag{3}$$

where $\boldsymbol{A}(\boldsymbol{q}) = [-\cos\beta \quad \cos\alpha\sin\beta \quad \sin\alpha\cos\beta \quad 0]$ and $\boldsymbol{q} = \left[x\ y\ z\ \beta\right]^{\mathrm{T}}$.

Suppose $\boldsymbol{S}(\boldsymbol{q}) \in R^{4\times 3}$ is a full rank matrix, which is a set of bases in the null space of $\boldsymbol{A}(\boldsymbol{q})$.We can obtain

$$\boldsymbol{A}(\boldsymbol{q})\boldsymbol{S}(\boldsymbol{q}) = 0 \tag{4}$$

In terms of (3) and (4), kinematics equation can been given by

$$\dot{\boldsymbol{q}} = \boldsymbol{S}(\boldsymbol{q})\boldsymbol{V} \tag{5}$$

where

$$\boldsymbol{S}(\boldsymbol{q}) = \begin{bmatrix} \sin\beta & 0 & 0 \\ \cos\alpha\cos\beta & -\sin\alpha & 0 \\ \sin\alpha\cos\beta & \cos\alpha & 0 \\ 0 & 0 & 1 \end{bmatrix} \text{ and } \boldsymbol{V} = [v_1, v_z, \omega_1]^T$$

where $\boldsymbol{V}$ denotes the velocity vector, v_1 is the line velocity of the climbing robot, ω_1 is the angular velocity of the rotating step motor, v_z is the motion velocity of the mechanical leg.

B. Dynamics Equation of the Climbing Robot

As shown in Fig. 1(b), the dynamic equation of the robot is expressed as

$$\begin{cases} \left(m_1+m_2\right)\dot{v}_{Y_1} = F_s - \left(m_1+m_2\right)g\sin\alpha\cos\beta \\ \left(m_1+m_2\right)\dot{v}_{Y_1} = \left(m_1+m_2+m_3\right)\dot{v}_{Z_1} \\ \left(m_1+m_2+m_3\right)\dot{v}_{Z_1} = F_n - F_a \\ \left(m_1+m_2\right)\dot{v}_{X_1} = 0 \\ I\ddot{\beta} = F_r r_1 \end{cases} \tag{6}$$

where m_1, m_2 and m_3 are the masses of the outer frame, synchronous leading screw and the inner frame of the climbing robot respectively. I is an inertia moment. v_{X_1}, v_{Y_1} and v_{Z_1} are velocities in the O_1X_1, O_1Y_1 and O_1Z_1 respectively, g is the gravity acceleration, $F_n = F_{n1} + F_{n2}$, $F_a = F_{a1} + F_{a2}$ are the total support force and the total adsorption force respectively.

C. Pneumatic System

Fig.2 shows the configuration of the pneumatic system which is used to control the cylinders and suckers. The adsorption force in the suckers can been adjusted to make the robot move smoothly and stably.

In Fig.2, the vacuum generator is used to produce the negative pressure. The gas inflow and outflow can be controlled by the opening and closing of high-frequency solenoid valves. As a result, the air flow in the suckers and cylinders can been controlled and adjusted.

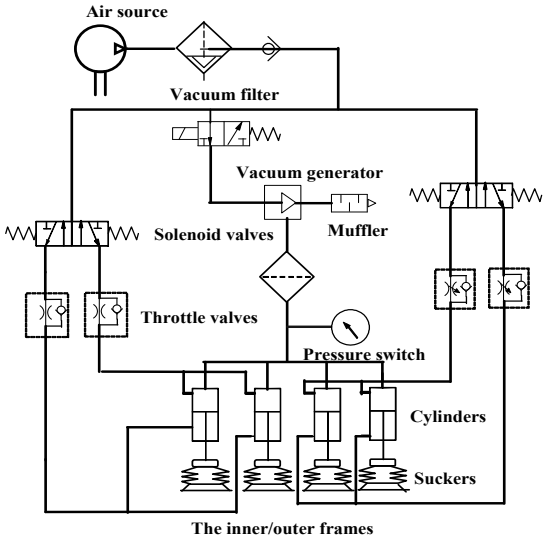

Fig. 2 The pneumatic system of the climbing robot.

Fig. 3 shows a sucker absorbing on a curved surface. When this sucker absorbs on the aircraft, it can be extended among the range of 5°-30°. Therefore, the robot can adsorb on the curved surface firmly.

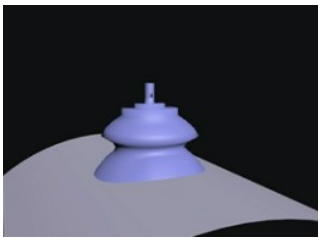

Fig.3 Suction cup absorbing on a curved surface.

D. Fuzzy Control of the Adsorption Force

The adsorption force controller is designed by using a fuzzy logic control(FLC). Fig. 4 illustrates the fuzzy control structure of adsorption force for the aircraft skin inspection robot, in which input and output are the desired pressure difference p_d and the actual pressure difference p in the suckers respectively, and the least squares support vector regression (LS-SVR) prediction model is designed as a feed-forward compensation control (SVR-FCC). FLC and SVR-FCC are implemented in a DSP controller, which is described in [10]-[11].

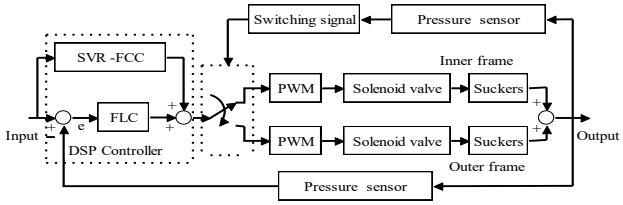

Fig. 4 Fuzzy control structure of pressure difference .

Firstly, the SVR prediction model between pressure difference and pulse width modulation (PWM) duty cycle in the adsorption system is established by using the good non-linear mapping ability of LS-SVR. The model can predict the expected pressure difference, then the predicted value is used as PWM signal in combination with the fuzzy control. Duty ratio d is used to control the action of the solenoid valve to regulate the adsorption force of the suckers. Switching signal $\sigma = 1$ denotes the inner frame , and $\sigma = 2$ denotes outer frame.

We briefly describe the LS-SVR algorithm[12]. Suppose a training sample set $\{x_i, y_i, i = 1,2,\cdots,N\}$, where $x_i \in R^n$ is the input vector and $y_i \in R$ is the desired output. In the higher dimensional feature space, the linear SVR model is given by

$$f(x) = \boldsymbol{w}^T \varphi(x) + b \tag{7}$$

where $\varphi(x)$ denotes the mapping from the input space to the feature space, $\boldsymbol{w}$ is a vector in the feature space, and b is the bias term.

The LS-SVR algorithm is used to solve the following optimal problem.

$$\begin{cases} \min J(w,\varepsilon) = \dfrac{1}{2}\| \boldsymbol{w} \|^2 + \dfrac{C}{2}\sum_{i=1}^{n} \varepsilon_i^2 \\ s.t. \quad y_i = f(x_i) = \boldsymbol{w}^T \varphi(x_i) + b + \varepsilon_i, \ i = 1,2\cdots n \end{cases} \tag{8}$$

where $J(w,\varepsilon)$ denotes the optimization objective function, ε_i denotes the relaxation factor, and C denotes the penalty factor.

The Lagrange multiplier method is as following:

$$L(\boldsymbol{w}, b, \varepsilon_i, a_i) = \frac{1}{2}\| \boldsymbol{w} \|^2 + \frac{C}{2}\sum_{i=1}^{n} \varepsilon_i^2 - \sum_{i=1}^{n} [a_i(\boldsymbol{w}^T \varphi(x_i) + b + \varepsilon_i - y_i] \tag{9}$$

where a_i (i = 1,2,.....n) is a Lagrange multiplier.

In terms of Karush-Kuhn-Tucker (KKT) conditions, the optimal solution of (9) can be given by

$$\boldsymbol{w} = \sum_{i=1}^{n} a_i \varphi(x_i), \ a_i = C\varepsilon_k, \ \sum_{i=1}^{n} a_i = 0, \ \boldsymbol{w}^T \varphi(x_i) + b + \varepsilon_i = y_i .$$

In nonlinear cases, the RBF kernel function can be used

$$K(x_i, x) = \exp(-\frac{\| x_i - x \|^2}{2\sigma^2}) \tag{10}$$

where σ is the width of the function.

The prediction function can be expressed as

$$f(x) = \sum_{i=1}^{n} a_i K(x_i, x) + b \tag{11}$$

In Fig.4, the two-dimension fuzzy controller is adopted. The deviation between the desired pressure difference and actual pressure difference, and the variation of the deviation value are taken as the inputs of the fuzzy controller. The outputs of the FLC and the SVR-FCC are added as the input of the PWM by the switching signal.

In the design of the FLC, fuzzy linguistic variables are selected as {NB,NM,NS,Z,PS,PM,PB}. According to the actual accuracy requirements, the universes of deviation value e, the variation of deviation value ec ,and the output are defined respectively as

$$E = \{-6,-5,-4,-3,-2,-1,0,1,2,3,4,5,6\},$$
$$EC = \{-3,-2,-1,0,1,2,3\},$$
$$U = \{-6,-5,-4,-3,-2,-1,0,1,2,3,4,5,6\}.$$

Parameters of the FLC are set as $e \in [-2\text{KPa}, 2\text{KPa}]$, $ec \in [-1,1]$, the quantization factors $K_e = 3$ and $K_{ec} = 3$, the proportion factor $K_u = 1$, $d \in [-0.06, 0.06]$. As shown in Fig.5, the membership functions of E , EC and U are selected as triangular functions with uniform distribution and non-uniform distribution respectively.

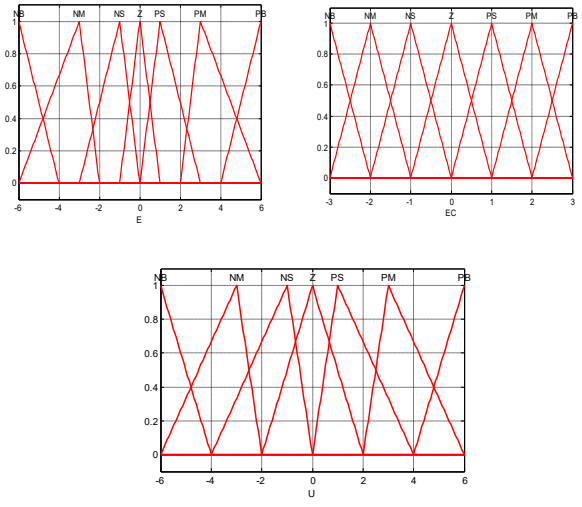

Fig.5 The membership functions of E , EC and U

The rule matrix for this fuzzy logic controller is shown in Table 1. This rule base is acquired based on the experience of controlling the adsorption force for the robot.

TABLE 1. FUZZY CNTROL RULES

EC	E						
	NB	NM	NS	Z	PS	PM	PB
NB	NB	NB	NM	NM	NS	PS	PM
NM	NB	NB	NM	NS	Z	PS	PM
NS	NB	NM	NS	Z	Z	PS	PM
Z	NB	NM	NS	Z	PS	PM	PB
PS	NM	NM	Z	Z	PS	PB	PB
PM	NM	NS	Z	PS	PM	PB	PB
PB	NM	NS	PS	PM	PM	PB	PB

III. SWITCHING MOTION EXPERIMENT

The weight of robot is 9.5kg.Volume flow of the vacuum generator is 60L/min. The robot moves on the fuselage at a speed of 0.5m/min and the pose of the robot is recorded in the movement of the robot by the pose sensor. The experimental results show that the climbing robot has a good switching performance between inner frame and outer frame, which is suitable for the change of the curvature on the aircraft surface.

A. Switching Motion Gaits

Fig. 6 shows the motion gaits of the robot moving on the fuselage.

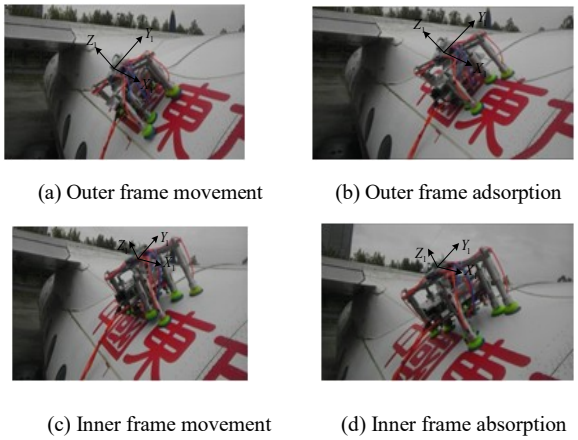

(a) Outer frame movement (b) Outer frame adsorption

(c) Inner frame movement (d) Inner frame absorption

Fig. 6 Switching motion gaits of the robot on the fuselage.

In the initial state, the suckers of the inner frame and outer frame adsorb on the surface of the aircraft. Then the suckers of the outer frame are released, the cylinders of the outer frame are lifted, and the outer frame slides along the Y_1-axis as shown in Fig. 6. When the outer frame moves nearly 25cm, the legs of outer frame drop down and suckers adsorb on aircraft surface. The robot motion is switched from outer frame to inner frame at this time. Finally, the robot completes one-step sliding gait through one switching movement on the plane surface. The experiment results of the above motion gait show that the climbing robot can adapt to the surface of the aircraft with curvature change when crawling on the surface of the aircraft. Fig.7 shows curves of the position and posture of the robot during the switching movement on the aircraft surface.

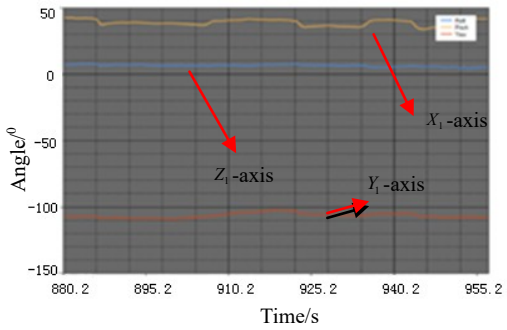

Fig. 7 Pose changes of the robot.

In Fig.7, the X_1-axis expresses the pitch angle; the Y_1-axis is the roll angle; the Z_1-axis is yaw angle. The robot completed one-step sliding movement from $880.2\,\mathrm{s}$ to $955.2\,\mathrm{s}$.The above experimental results of the switching movement gaits show that the climbing robot can better adapt to the curvature change of the aircraft. It is verified that the design of the double frame for the robot is feasible.

B. Fuzzy control of Pressuree Difference

Firstly, the SVR prediction model is trained by using the data of pressure difference and duty ratio of suckers collected in experiment. The duty ratio of PWM signal is used as the output of the SVR model, and the pressure difference of suckers is used as the input. The pressure difference and duty ratio of suckers corresponding to different PWM duty ratios were obtained by training samples. Nine groups of training samples and six groups of predictive data were collected. In terms of cross-validation, the width range of RBF kernel σ^2 and parameters C, ε are set as 2.8 ,1, and 0.001, respectively. The prediction result was shown in Fig.8, which showed the normalized pressure difference p and the normalized duty cycle d. The mean squared error(MSE) of the predicting samples is used to evaluate the modeling accuracy. MSE is defined as following

$$MSE = \frac{1}{n}\sum_{k=1}^{n}(y_k - \hat{y}_k)^2 \tag{12}$$

where n is the number of predicting samples, y_k is the real value for the duty cycle of the PWM signal, and $\hat{y}_k$ is the predicted value. The MSE of prediction samples is 0.00068. The result of the prediction experiment shows that the proposed prediction method has good prediction accuracy. The SVR prediction model achieves the best performance. Therefore, the LS-SVR model can be used as the feed-forward compensation controller of the adsorption force.

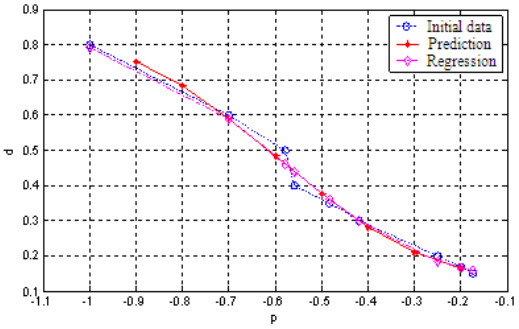

Fig.8 Prediction result of SVR model.

Fig.9 shows the change curve of pressure difference at $p_d = -17\mathrm{KPa}$. Because there exit different curvatures of the aircraft surface, the pressure difference of the suckers can been judged by checking attitude angle of the robot so as to adjust the sucker's adsorption force. Compared with SVR-FCC , the FLC+SVR-FCC can better adjust the pressure difference of the suckers to reach the desired value to overcome disturbance and noises, and the pressure difference almost reaches a stable state after about 1 s. If the pressure difference changes from -17KPa to -12KPa in a stable state, it may cause the robot to slip from the aircraft surface due to insufficient adsorption force. Therefore, the fuzzy control of the adsorption force can be used for self-regulation control of sucker adsorption.

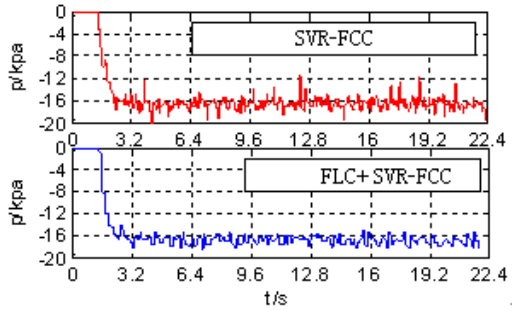

Fig. 9 Change curves of pressure difference at $p_d = -17\mathrm{KPa}$.

C. Image Inspection of Rivet Damage

The image acquisition and processing software in the ground computer was designed. In the above switching motion test, the climbing robot collects the images of rivet damage on the surface of the aircraft in real time by carrying the CCD camera, and sends it to the skin inspection system through the wireless transmission equipment, and then the image processing was carried out. Fig.10 is the dynamic detection of rivet images during the switching process of the inner and outer frames of the robot. The detection of rivet edge by Canny operator is rough, and the contour is not clear and obvious, and contains the noise signal. Therefore, in order to further improve the effect of edge detection, the circle detection algorithm by Hough transform was used. It can be seen that a clearer edge contour of the rivet was obtained during the switching movement. The non-destructive test results showed that the climbing robot can obtain smooth and clear inspection results.

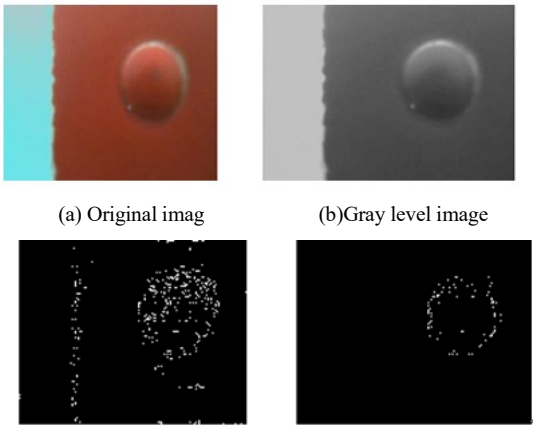

(a) Original imag (b)Gray level image

(c) Edge detection (d) Circle detection

Fig. 10 Rivet detection during switching movement.

IV. CONCLUSION

In this paper, the structure of the climbing robot with double frame for skin inspection is described. The motion constraint and dynamics equation are established. In order to improve the stability of the pressure difference in the suckers, the absorption force control combining the fuzzy control and the feed-forward compensation control using the SVR prediction model is proposed. The experiments of the movement, absorption force and the non-destructive inspection for the robot on the aircraft skin surface were carried out. The motion control and adsorption control can been realized with high stability for the climbing robot. Finally, the effectiveness of the rivet inspection is illustrated.

ACKNOWLEDGMENT

This work was supported by the National Natural Science Foundation of China (Grant No. 61573185) and JiangSu Scientific Support Program of China (Grant No. BE2010190).

REFERENCES

[1] Yu, Seung Nam, J. H. Jang, and C. S. Han, “Auto Inspection System Using a Mobile Robot for Detecting Concrete Cracks in a Tunnel,” Automation in Construction,2007,pp.255–261.

[2] Mahmoud Tavakoli, Carlos Viegas, Lino Marques, J. Norberto Pires and An´ıbal T. de Almeida, “OmniClimber-II: An omnidirectional Climbing Robot with High Maneuverability and Flexibility to Adapt to Non-flat Surfaces,” IEEE International Conference on Robotics and Automation , Karlsruhe, Germany, May 6-10, 2013,pp.1349–1354.

[3] Mel Siegel and Priyan Gunatilake, “Remote Enhanced Visual Inspection of Aircraft by a Mobile Robot,”1998 IEEE Workshop on Emerging Technologies, Intelligent Measurement and Virtual Systems for Instrumentation and Measurement - ETIMVIS’98 St. Paul, MN, USA, May,pp. 15–16.

[4] C. J Alberts, C. W. Carroll , W. M. Kaufman, C. J. Perlee , and M. Siegel,“Automated Inspection of Aircraft,”Technical report,DOT/FAA/AR-97/69, Carnegie Mellon Research Institute, Pittsburgh, USA. 1998,pp.15230–2950.

[5] C.Deneke, C. Schlosser, S. Mehler, and T. Schuppstuhl,“Positioning NDT Sensors with Mobile Robot for Efficient Aircraft Inspections ,” 7th International Symposium on NDT in Aerospace,2015,pp.1–8.

[6] C. Schlosser and T. Schuppstuhl. Numerical Controlled Robot Crawler: New Resource for Industries with Large Scale Products, Production Engineering Research and Development. vol. 8, 2014, pp.719–725.

[7] José Sánz, Manuel Ferre, Alvaro Espada, Matias Collar Narocki, and José Fernández Pard,“Robotized Inspection System of the External Aircraft Fuselage based on Ultrasound,” The 2010 IEEE/RSJ International Conference on Intelligent Robots and Systems, Taiwan:Taipei, 2010,pp.18–22.

[8] Ming-Shaung Ju, Chou-Ching K. Lin, Dong-Huang Lin, Ing-Shiou Hwang, and Shu-Min Chen,“A Rehabilitation Robot With Force-Position Hybrid Fuzzy Controller: Hybrid Fuzzy Control of Rehabilitation Robot,” IEEE Transactions on Neural Systems and Rehabilitation Engineering,vol.12,no.6, 2005, pp.349-358.

[9] Amitava Chatterjee, Ranajit Chatterjee,“Augmented Stable Fuzzy Control for Flexible Robotic Arm Using LMI Approach and Neuro-Fuzzy State Space Modeling,”IEEE Transactions on Industrial Electronics,vol.55,No.3 2008,pp.1256-1270.

[10] Jiayue Gu, Congqing Wang and Xuewei Wu, “Self-adjusted Adsorption Strategy for an Aircraft Skin Inspection Robot,” Journal of Mechanical Science and Technology, vol.32,no.6,2018, pp. 2867–2875.

[11] Jiayue Gu, Congqing Wang, “The Adsorption Force Self-Adjustment for the Aircraft Skin Inspection Robot with Double Frame,” Proceedings of the 36th Chinese Control Conference,Dalian,China, 2017,pp.6708–6713.

[12] Cristianini Nello and Shawe-Taylor John, “ An Introduction to Support Machines and Other Kernel-based Learning Methods,”England, Cambridge University Press 2000.